J|A|C|S
ARTICLES
Published on Web 12/10/2005

Surface Modification of Confined Microgeometries via Vapor-Deposited Polymer Coatings

Hsien-Yeh Chen, Yaseen Elkasabi, and Joerg Lahann*

Contribution from the Departments of Chemical Engineering, Materials Science and Engineering, and Macromolecular Science and Engineering, University of Michigan, Ann Arbor, Michigan 48109

Received October 24, 2005; E-mail: lahann@umich.edu

Abstract: The development of generally applicable protocols for the surface modification of complex substrates has emerged as one of the key challenges in biotechnology. The use of vapor-deposited polymer coatings may provide an appealing alternative to the currently employed arsenal of surface modification methods consisting mainly of wet-chemical approaches. Herein, we demonstrate the usefulness of chemical vapor deposition polymerization for surface modification in confined microgeometries with both nonfunctionalized and functionalized poly(*p*-xylylenes). For a diverse group of polymer coatings, homogeneous surface coverage of different microgeometries featuring aspect ratios as high as 37 has been demonstrated based on optical microscopy and imaging X-ray photoelectron spectroscopy. In addition, height profiles of deposited polymer footprints were obtained by atomic force microscopy and imaging ellipsometry indicating continuous transport and deposition throughout the entire microchannels. Finally, the ability of reactive coatings to support chemical binding of biological ligands, when deposited in previously assembled microchannels, is demonstrated, verifying the usefulness of the CVD coatings for applications in micro/nanofluidics, where surface modifications with stable and designable biointerfaces are essential. The fact that reactive coatings can be deposited within confined microenvironments exhibits an important step toward new device architectures with potential relevance to bioanalytical, medical, or "BioMEMS" applications.

Introduction

Defined and stable surface properties along with the capability to immobilize active biomolecules onto a surface are key features for the development of miniaturized biodevices, such as micro total analysis systems (μTAS),[1] microfabricated cell sorters,[2] microseparators for DNA[3,4] and proteins,[5−7] cell-based assays,[8] and embryonic patterning networks.[9] In such miniaturized high-tech systems, very large surface-to-volume ratios are typically encountered creating a situation where slight inhomogeneities in the surface chemistry will cause device malfunction.[10] The development of advanced surface modification protocols that are equally applicable to flat and three-dimensional surfaces has accordingly emerged as one of the critical challenges for many biotechnology applications. From a device design perspective, poly(dimethylsiloxane) (PDMS) is often discussed as the prime candidate material for microfluidic systems because of its favorable mechanical properties[11,12] and its straightforward manufacturing by rapid prototyping.[13] However, PDMS is a very hydrophobic polymer, has undefined surface properties, and promotes nonspecific protein adhesion.[14] In addition, the absence of functional groups at the PDMS surface prevents covalent immobilization of proteins, enzymes, or antibodies. To reduce these adverse properties of PDMS, several methods including graft polymerization,[15−17] plasma treatment,[18] UV/ozone treatment,[19] silanization,[20] adsorption of detergents,[14] proteins,[21] and polyelectrolytes[22] have been used to modify PDMS but often show hydrophobic

(1) Berg, A.; Olthius, W.; Bergveld, P. *Micro Total Analysis Systems 2000*; Kluwer Academic Publishers: Dordrecht, The Netherlands, 2000.
(2) Fu, A. Y.; Spence, C.; Scherer, F. H.; Arnold, F. H.; Quake, S. R. *Nat. Biotechnol.* **1999**, *17*, 1109−1111.
(3) Burns, M. A.; Johnson, B. N.; Brahmasandra, S. N.; Handique, K.; Webster, J. R.; Krishnan, M.; Sammarco, T. S.; Man, P. M.; Jones, D.; Heldsinger, D.; Mastrangelo, C. H.; Burke, D. T. *Science* **1998**, *282*, 484−487.
(4) Effenhauser, C. S.; Bruin, J. M.; Paulus, A.; Ehrat, M. *Anal. Chem.* **1997**, *69*, 3451−3457.
(5) Huber, D. L.; Manginell, R. P.; Samara, M. A.; Kim, B. I.; Bunker, B. C. *Science* **2003**, *301*, 352−354.
(6) Mao, H.; Yang, T.; Cremer, P. S. *Anal. Chem.* **2002**, *74*, 379−385.
(7) Chen, S. H.; Sung, W. C.; Lee, G. B.; Lin, Z. Y.; Chen, P. W.; Liao, P. C. *Electrophoresis* **2001**, *22*, 3972−3977.
(8) Li, P.; Harrison, D. J. *Anal. Chem.* **1997**, *69*, 1564−1568.
(9) Lucchetta, E. M.; Lee, J. H.; Fu, L. A.; Patel, N. H.; Ismagilov, R. F. *Nature* **2005**, *434*, 1134−1138.
(10) Li, Y.; Phohl, T.; Kim, J. H.; Yasa, M.; Wen, Z.; Kim, M. W.; Safina, C. R. *Biomed. Microdevices* **2001**, *3*, 239−244.
(11) Quake, S. R.; Scherer, A. *Science* **2000**, *24* (290), 1536−1540.
(12) Johnson, T. J.; Ross, S.; Gaitan, M.; Locascio, L. E. *Anal. Chem.* **2001**, *73*, 3656−3661.
(13) Duffy, D. C.; MacDonald, J. C.; Schueller, O. J. A.; Whitesides, G. A. *Anal. Chem.* **1998**, *70*, 4974−4984.
(14) Linder, V.; Verpoorte, E.; Thormann, W.; de Rooij, N. F.; Sigrist, H. *Anal. Chem.* **2001**, *73*, 4181−4189.
(15) Hu, S.; Ren, X.; Bachman, M.; Sims, C. E.; Li, G. P.; Allbritton, N. L. *Anal. Chem.* **2004**, *76*, 1865−1870.
(16) Hu, S.; Ren, X.; Bachman, M.; Sims, C. E.; Li, G. P.; Allbritton, N. L. *Anal. Chem.* **2002**, *74*, 4117−4123.
(17) Hu, S.; Ren, X.; Bachman, M.; Sims, C. E.; Li, G. P.; Allbritton, N. L. *Langmuir* **2004**, *20*, 5569−5574.
(18) Duffy, D. C.; Mcdonald, J. C.; Schueller, O. J. A.; Whitesides, G. M. *Anal. Chem.* **1998**, *70*, 4974−4984.
(19) Berdichevsky, Y.; Khandurina, J.; Guttman, A.; Lo, Y.-H. *Sens. Actuators, B* **2004**, *97*, 402−408.
(20) Grzybowski, B. A.; Haag, R.; Bowden, N.; Whitesides, G. M. *Anal. Chem.* **1998**, *70*, 4645−4652.
(21) Yang, T. L.; Jung, S. Y.; Mao, H. B.; Cremer, P. S. *Anal. Chem.* **2001**, *7*, 165−169.

10.1021/ja057082h CCC: $33.50

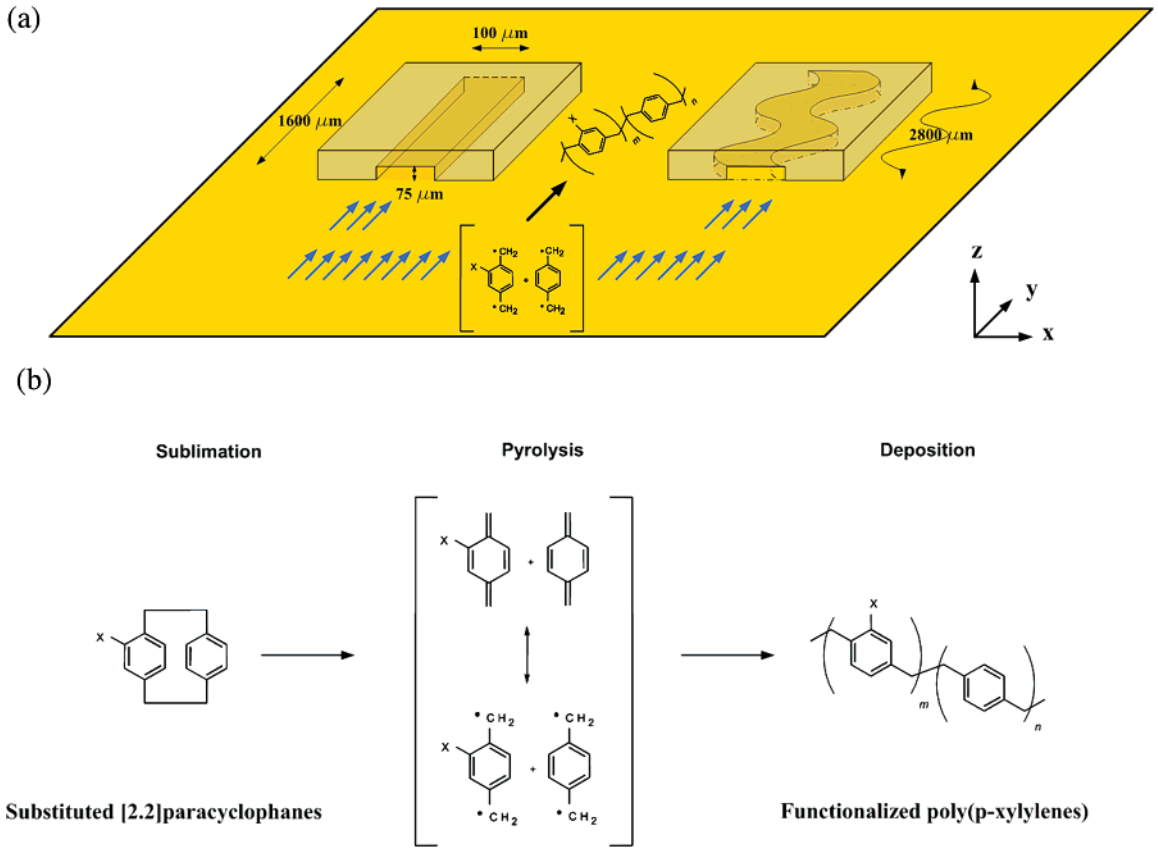

functionalized poly(*p*-xylylenes)	1	2	3	4	5	6	7
X =	—NH_2	CF_3	C_2F_5	C_6F_5	C_6H_5	—Cl	—H

Figure 1. (a) Chemical vapor deposition polymerization within confined geometries of straight and meandering channels. (b) Functionalized poly(*p*-xylylenes) prepared via chemical vapor deposition polymerization used in this study.

recovery of PDMS and loss of protein resistance with time hampering their use for long-term applications.[23]

Deposition of thin polymer films to establish chemically defined interfaces offers a unique way to overcome these limitations. Recently, we reported a widely applicable surface modification approach based on chemical vapor deposition (CVD) polymerization[24,25] to deposit *reactive coatings* on the luminal surface of open PDMS-based microchannels.[26] In addition to being compatible with the requirements of biological assays, these coatings provide a designable interlayer that is stable under the conditions of bioassays.[26,27] The *reactive coatings* are based on polymers known as functionalized poly(*p*-xylylenes), which establish interfaces equipped with chemically reactive groups that can be selected from a variety of different chemical species, including amines, alcohols, aldehydes, activated carboxylic acids, and anhydrides.[25,28] *Reactive coatings* have been useful for immobilization of biomolecules,[29,30] planar cell and protein patterning,[31,32] and for patterning of polymer brushes[32,33] on freely accessible substrates. However, the appropriate question of whether the concept of CVD polymerization is expandable to the coating of complex microgeometries with high aspect ratios or is only applicable to cases where the individual pieces are modified prior to assembly remains open.[15] If CVD polymerization indeed could be applied to previously assembled devices, the scope of practical use could be significantly widened. In this report, we will demonstrate—for the first time—that CVD polymerization can be used to deposit a range of functionalized poly(*p*-xylylenes) within confined microgeometries (Figure 1).

(22) Barker, S. L. R.; Tarlov, M. J.; Canavan, H.; Hickman, J. J.; Locascio, L. E. *Anal. Chem.* **2000**, *72*, 4899−4903.
(23) Makamba, H.; Kim, J. H.; Lim, K.; Park, N.; Hahn, J. H. *Electrophoresis* **2003**, *24*, 3607−3619.
(24) Lahann, J.; Klee, D.; Hocker, H. *Macromol. Rapid Commun.* **1998**, *19*, 441−444.
(25) Lahann, J.; Langer, R. *Macromolecules* **2002**, *35*, 4380−4386.
(26) Lahann, J.; Balcells, M.; Lu, H.; Rodon, T.; Jensen, K. F.; Langer, R. *Anal. Chem.* **2003**, *75*, 2117−2122.
(27) Chen, H.-Y.; Lahann, J. *Anal. Chem.* **2005**, *77*, 6909−6914.
(28) Nandivada, H.; Chen, H.-Y.; Lahann, J. *Macromol. Rapid Commun.* **2005**, *26*, 1794−1799.
(29) Lahann, J.; Klee, D.; Pluester, W.; Hoecker, H. *Biomaterials* **2001**, *22*, 817−826.
(30) Lahann, J.; Pluster, W.; Rodon, T.; Fabry, M.; Klee, D.; Gattner, H. G.; Hocker, H. *Macromol. Biosci.* **2002**, *2*, 82−87.
(31) Lahann, J.; Balcells, M.; Rodon, T.; Lee, J.; Choi, I. S.; Jensen, K. F.; Langer, R. *Langmuir* **2002**, *18*, 3632−3638.
(32) Lahann, J.; Choi, I. S.; Lee, J.; Jensen, K. F.; Langer, R. *Angew. Chem., Int. Ed.* **2001**, *40*, 3166−3169.
(33) Lahann, J.; Langer, R. *Macromol. Rapid Commun.* **2001**, *22*, 968−971.

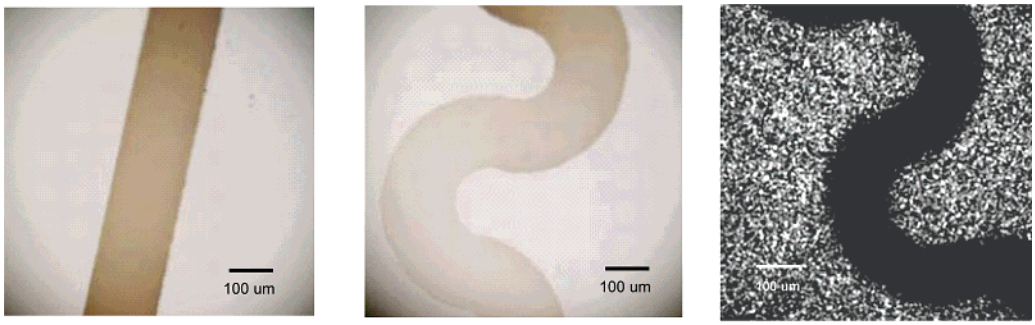

Figure 2. (a, b) Optical micrographs showing poly(*p*-xylylene) (**7**) films deposited within microchannels. (c) XPS mapping (Si_{2p}, 99.0 eV) of poly(*p*-xylylene) films deposited within microchannels. All images were taken after CVD coating in confined microgeometries and subsequent removal of the PDMS molds for imaging purposes.

Results and Discussions

CVD Polymerization in Enclosed Microchannels. To create a general understanding of the phenomenon of CVD polymerization within confined microgeometries, seven different poly(*p*-xylylenes) were deposited via CVD polymerization within both removable and sealed PDMS microchannels.[34] A subgroup of five poly(*p*-xylylenes), polymers **1**−**5**, had reactive side group (so-called reactive coatings), while two commercially available poly(*p*-xylylenes) were included as nonfunctionalized references (polymers **6** and **7**). The CVD polymerization process used for coating of the microfluidic channels with both reactive coatings and nonfunctionalized coatings is an adaptation of the commercially exploited Gorham process,[35] routinely practiced for the deposition of polymer coatings marketed as parylenes. As shown in Figure 1, functionalized [2.2]paracyclophanes are first sublimed, and the resulting vapor is transferred into the pyrolysis zone. Through control of the polymerization parameters, such as sublimation and pyrolysis temperatures, pressure, and mass flow, selective cleavage of C−C bonds can be obtained.[36] While quantitative conversion into the corresponding *p*-quinodimethanes is critical for CVD polymerization,[25] care must be taken to avoid decomposition of the functional groups under the conditions of thermal activation. The selection of process parameters must account for this balance between activation, i.e., the opening of the aliphatic bridges of the [2.2]paracyclophanes, and the avoidance of thermally induced side reactions. The PDMS microchannels used in this study were open at both ends and had the following dimensions: 75 μm high and 100 μm wide. Both straight (1600 μm long) and meandering channel (2800 μm long) layouts with high aspect ratios were studied. While high aspect ratios are often encountered in miniaturized bioanalytical devices, their homogeneous surface modification can be challenging. After removal of the PDMS mold, the footprint of the deposited films remained on the silicon substrates as confirmed by optical microscopy. In parts a and b of Figure 2, optical micrographs of a silicon substrate coated with polymer **7** are shown for both straight and meandering microchannels. While the deposited polymer films were thicker in the inlet and outlet region of the microchannels than in the center, the micrographs clearly indicate deposition of polymer **7** throughout the entire microchannel. To verify that the contrast in the micrographs is indeed due to the vapor-deposited coating, we examined the footprints of polymer **7** on the silicon substrate using XPS in the imaging mode. This technique enables spatially resolved mapping of the elemental distribution of reporter atoms on a surface. Figure 2c shows the elemental composition map of silicon recorded for a 600 × 600 μm^2 area of a meandering channel coated with polymer **7**. Silicon is a characteristic atom of the substrate used in this study, a silicon wafer, and is not present in polymer coating **7**. As anticipated, the composition map confirms that silicon is only detectable for areas that were masked during CVD polymerization, while the entire microchannel footprint is devoid any detectable amounts of silicon. Based on this finding we concluded that the entire microchannel is covered with a homogeneous film of polymer **7**, which must be thicker than the information depth of XPS (about 10 nm).[37] Correspondingly, a homogeneous distribution of carbon was detected throughout the entire footprint of the microchannel but not for the areas masked during CVD polymerization (see the Supporting Information). Taken together, the data obtained by optical microscopy and imaging XPS suggest that CVD polymerization can be used to deposit homogeneous polymer films within confined geometries, such as the straight and meandering microchannels used in this study.

Deposition of Reactive Coatings in Enclosed Microchannels. Once the fundamental feasibility of CVD polymerization within previously assembled microdevices was demonstrated for the nonfunctionalized poly(*p*-xylylene) **7**, we extended our study to reactive CVD coatings **1**−**5**. For comparison, CVD polymerization was again conducted in straight and meandering microchannel geometries and film thicknesses were quantified with atomic force microscopy (AFM) and/or ellipsometry. In all cases, the CVD polymerization of [2.2]paracyclophanes resulted in transparent and topologically uniform polymer films. Moreover, the footprints of the reactive coatings deposited within the microchannels were typically detectable by optical microscopy. The ability to visualize the footprints of the coatings enabled us to extract height profiles at the interface between polymer coating using AFM in the tapping mode (Figure 3). The AFM study revealed height profiles for polymers **1**, **2**, **3**, **6**, and **7** (Table 1). In case of polymers **4** and **5** however, the deposited films were substantially thinner and the boundary between film and substrate was no longer observable by light

(34) McDonald, J. C.; Whitesides, G. M. *Acc. Chem. Res.* **2002**, *35*, 491−499.
(35) Gorham, W. F. *J. Polym. Sci., Polym. Chem. Ed.* **1966**, *4*, 3027−3039.
(36) Greiner, A.; Mang, S.; Schäfer, O.; Simon, P. *Acta Polym.* **1997**, *48*, 1−15.
(37) Briggs, D. *Surface Analysis of Polymers by XPS and Static SIMS*; Cambridge University Press: Cambridge, UK, 1998.

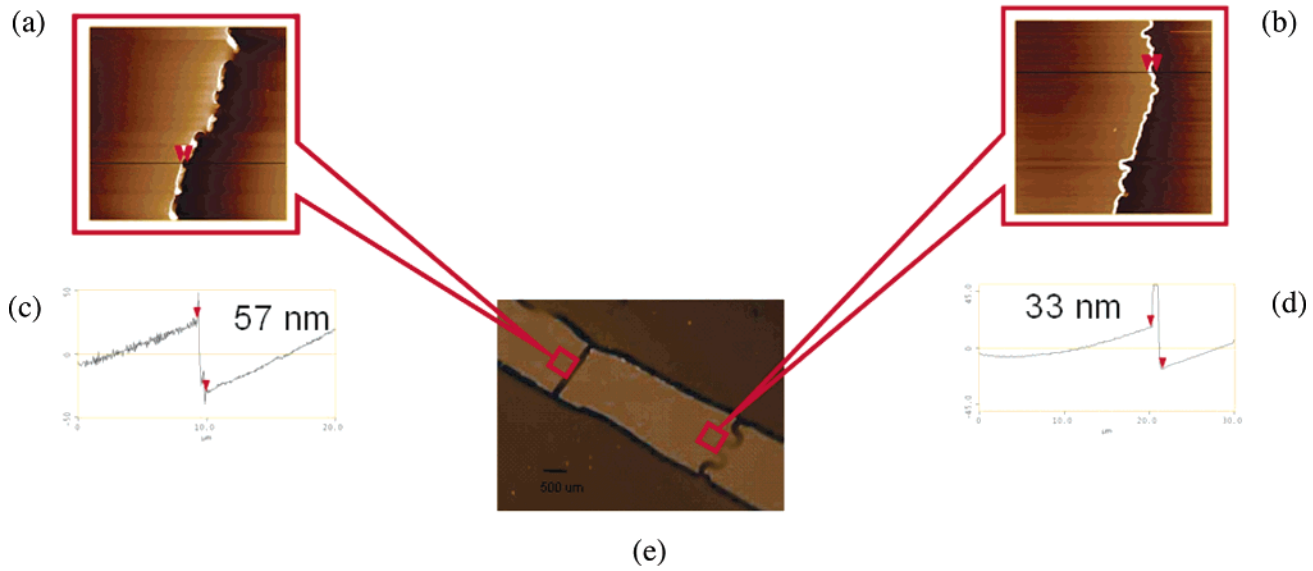

Figure 3. AFM cross section height analysis of (a) straight and (b) meandering channels of a substrate coated with CVD polymer **3**. The scanning size is 20 μm by 20 μm. (c, d) Corresponding height profiles revealing 57 nm film thickness for the straight channel and 33 nm for the meandering channel; (e) matching photograph taken by a digital camera.

Table 1. Film Thickness Characterization

polymer	film thickness (h_0) outside the channels (nm)[a]	film thickness (h_1) at straight channels (nm)[b]	degree of deposition at straight channels (%)[c]	film thickness (h_2) at meandering channels (nm)[b]	degree of deposition at meandering channels (%)
1	103	16	16	9	9
2	127	113	89	74	58
3	70	57	81	33	47
4	437	6[d]	1.4	5[d]	1.1
5	524	5[d]	1.0	2[d]	0.4
6	59	46	80	24	41
7	38	33	86	16	42

[a] Based on ellipsometry. [b] If indicated, otherwise the reported values are based on AFM. [c] Degree of deposition (%) = [h_1(or h_2)/h_0] × 100%. [d] Based on ellipsometry.

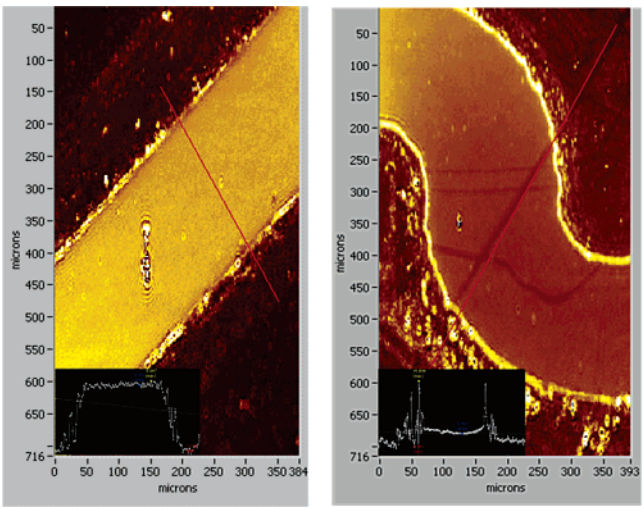

Figure 4. Cross section height analysis by imaging ellipsometry at straight and meandering channels coated with CVD polymer. CVD polymer **4** is shown as an example.

microscopy making it difficult to use AFM for height profiling. In these cases, we used imaging ellipsometry to unambiguously confirm the presence of the polymer films throughout the microchannel footprint. Figure 4 shows ellipsometric thickness maps recorded for polymer **4** on both straight and meandering microchannels. A clearly observable contrast between areas coated with the polymer film and the Si substrate is revealed by imaging ellipsometry. Quantitative height profiles were obtained from the ellipsometric data shown in Figure 4 indicating a thickness of 6 nm for the straight microchannel and 5 nm for the meandering microchannel, respectively. Prior to this experiment, the usefulness of imaging ellipsometry for thickness determination of ultrathin polymer films was validated by comparing the thickness of the same sample of polymer **1** measured by AFM and imaging ellipsometry. Within the margins of error, the thicknesses measured by AFM and imaging ellipsometry were identical demonstrating the usefulness of imaging ellipsometry for surface analysis of ultrathin CVD films. Throughout this series of experiments, film thicknesses measured at the center of the microchannel footprints were compared to film thicknesses measured for unconfined substrates, that is, open surfaces distant to the microchannels. Table 1 summarizes the complete set of thickness data for polymers **1**−**7**. Under the conditions of CVD polymerization, substantially different thicknesses were observed ranging from 38 nm measured for polymer **7** to 524 nm for polymer **5**. The film thickness was mainly determined by the amount of a given [2.2]paracyclophane used for CVD polymerization. Based on the thickness data, we were able to extract the degree of deposition for each polymer, being defined as the ratio of film thicknesses measured at the center of the microchannel and at the open substrate. In essence, this ratio indicates how effective a CVD coating can be deposited in the confined geometry. The deposition degree

will be 100% for a coating that is not limited by the confinement imposed by the microchannel geometry. Although we intuitively expected the deposition degree to be independent from the film thickness, we verified this relationship by depositing films of polymer **1** with various thicknesses and measured the corresponding degrees of deposition. For both straight and meandering microchannels the degree of deposition was constant and did not change with increasing film thickness. Assuming the constant trends observed for reactive coating **1** to be similar for the entire group of poly(*p*-xylylenes) enables comparison of polymer coatings with substantially different deposition degrees (Table 1). Polymers **1**, **4**, and **5** showed relative low deposition degrees, ranging from 1% to 16% for straight microchannels and from 0.4% to 9% for meandering channels. In contrast, polymers **2**, **3**, **6**, and **7** had deposition degrees higher than 80% for the straight microchannel geometry and above 40% for the meandering microchannel geometry. The substantial differences in deposition rate between different poly(*p*-xylylenes) is not well understood yet but may be—at least partially—due to (i) the different vapor pressures of the corresponding quinodimethanes and (ii) the different electronic effects that the functional groups may exhibit on the conjugated precursors. The differences between both layouts may be explained with (i) the curved layout of the microchannels and (ii) the 1.75 times longer pathway of the meandering microchannels as compared to that of the straight microchannels (meandering channels have a aspect ratio of 37 compared to 21 for straight channels). It is important to note that the actual thickness of the deposited reactive coatings is less critical to a given surface modification application, as long as the deposition of the polymer film occurs homogeneously throughout the microchannel and the resulting coatings still provide functional groups for further modification. With the homogeneous deposition of functionalized and nonfunctionalized poly(*p*-xylylenes) in confined geometries confirmed, we moved our focus toward the assessment of the ability of reactive coatings to support subsequent surface reactions, when deposited in complex microgeometries. In principle, the polymer coatings can then provide anchoring groups on the channel walls for the linkage of biomolecules.

Chemical and Biological Activity of Reactive Coatings Deposited onto the Luminal Surface of Enclosed Microchannels. To address the question of whether polymer films deposited within microchannels still maintain their typical reactivity toward corresponding binding partners, we conducted a series of immobilization studies with permanently sealed PDMS devices[34] after CVD polymerization. The microchannels were coated with polymers **1** or **2** prior to immobilization. While polymer **1** provides primary amino groups for coupling with activated carboxyl groups (amide formation), polymer **2** has keto groups that can react with hydrazines or hydrazides. To assess the chemical activity of both reactive coatings, PFP-derived biotin ligands **8** and hydrazide-derived biotin ligands **9** were used.[28] These ligands were chosen because they undergo nearly quantitative conversion with amines or ketones, respectively. Moreover, the interactions between biotin and streptavidin result in tight confinement of streptavidin on the biotin-modified surface, which can be exploited for visualization of ligand binding. Scheme 1 illustrates the surface modification approach used in this study based on the example of reactive coating **2**. For all ligand immobilization reactions, aqueous solutions of

Scheme 1. Immobilization Reactions Used for the Chemical Immobilization of Biotin and Subsequent Binding of Streptavidin onto Reactive Coating **2**

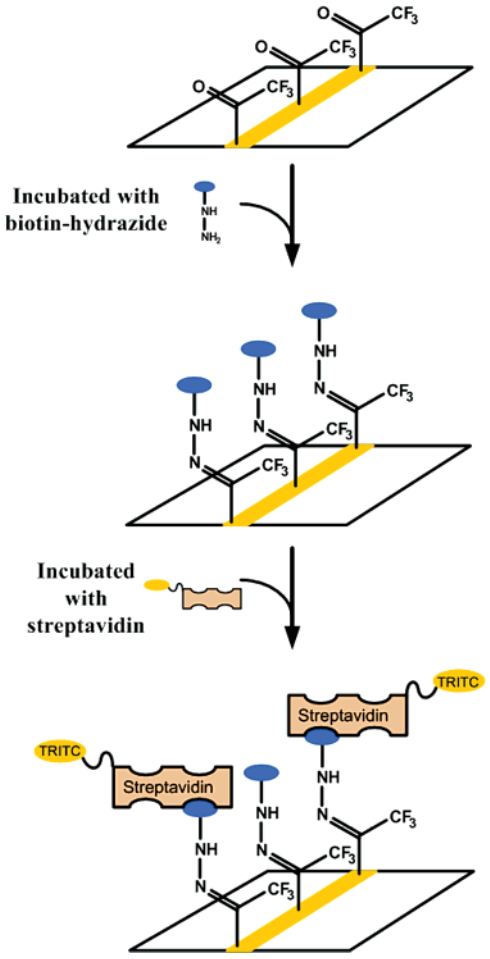

the corresponding biotin derivative were filled into the sealed microchannels of either meandering or straight geometry. After incubation for 60 min (5 min for hydrazide-derived biotin ligands), nonreacted ligands were washed away.

To examine the immobilization of biotin ligands within the microchannels (Scheme 2), we allowed rhodamine (TRITC)-conjugated streptavidin to bind to the biotin-modified surfaces. After thorough rinsing with buffer, the surfaces were visualized by fluorescence microscopy. Figure 5 shows microchannels that were coated with polymer **1** and then subjected to the biotin/strepdavidin protocol. Homogeneous distribution throughout the entire microchannel was observed, indicating that amino groups were available throughout the entire coating area. Similarly, the corresponding biotin ligands bound homogeneously to polymer **2**, as shown in Figure 6. Similar to the situation observed for polymer **1**, this finding indicates homogeneous reactivity of the deposited polymer films. This phenomenon appears to be independent of the observed thickness, because reactive coating **4** had one of the lowest degrees of deposition of all polymers included in this study (Figure S2 in the Supporting Information). The ability to deposit polymer coating with a relatively homogeneous distribution of reactive binding sides throughout the microchannel will be a critical feature when using reactive coatings to tailor surface properties of microchannels toward the needs of specific biological applications. While CVD

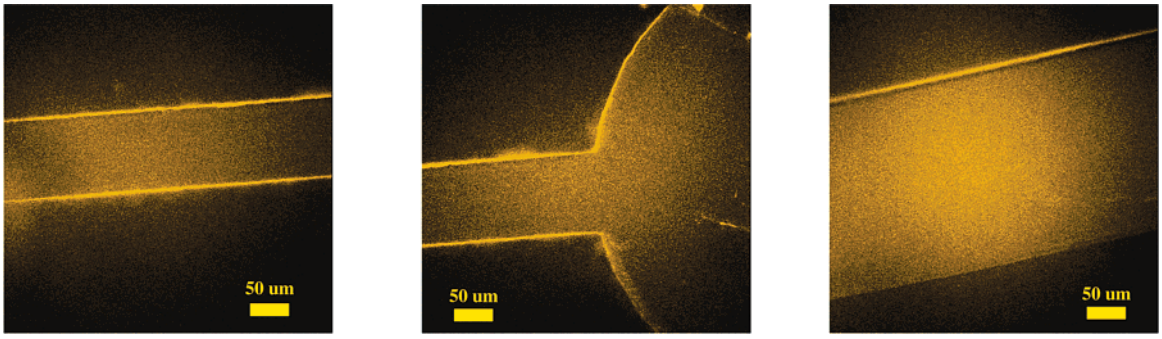

Figure 5. Fluorescence micrographs of sealed devices coated with reactive coating **1** after immobilization of PFP−biotin and self-assembly of TRITC-conjugated streptavidin. Examples are shown in different geometries with 75 μm depth and 100−300 μm width or 500 μm diameter.

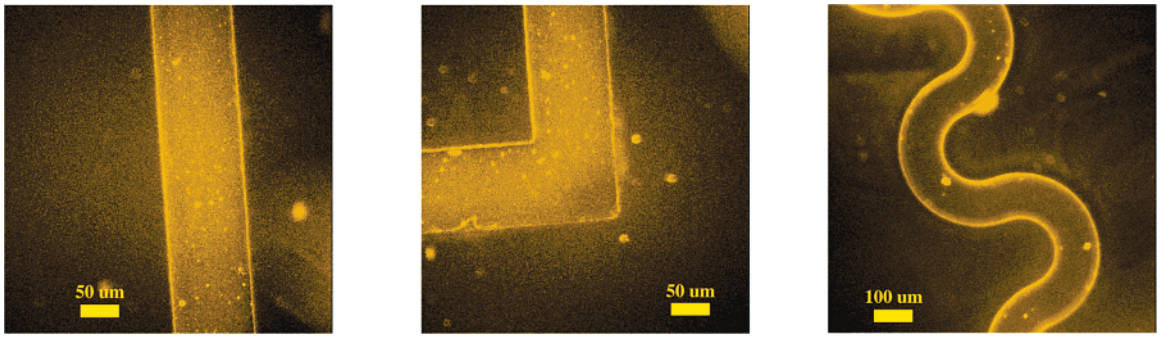

Figure 6. Fluorescence micrographs of sealed devices coated with reactive coating **2** after immobilization of hydrazide−biotin and self-assembly of TRITC-conjugated streptavidin. Examples are shown in different channel geometries of 75 μm depth and 100 μm width.

Scheme 2. Three-Dimensional Immobilization Protocol Used for the Surface Modification of the Surface Area of the Microchannels, as Shown for the Example of Reactive Coating **2**

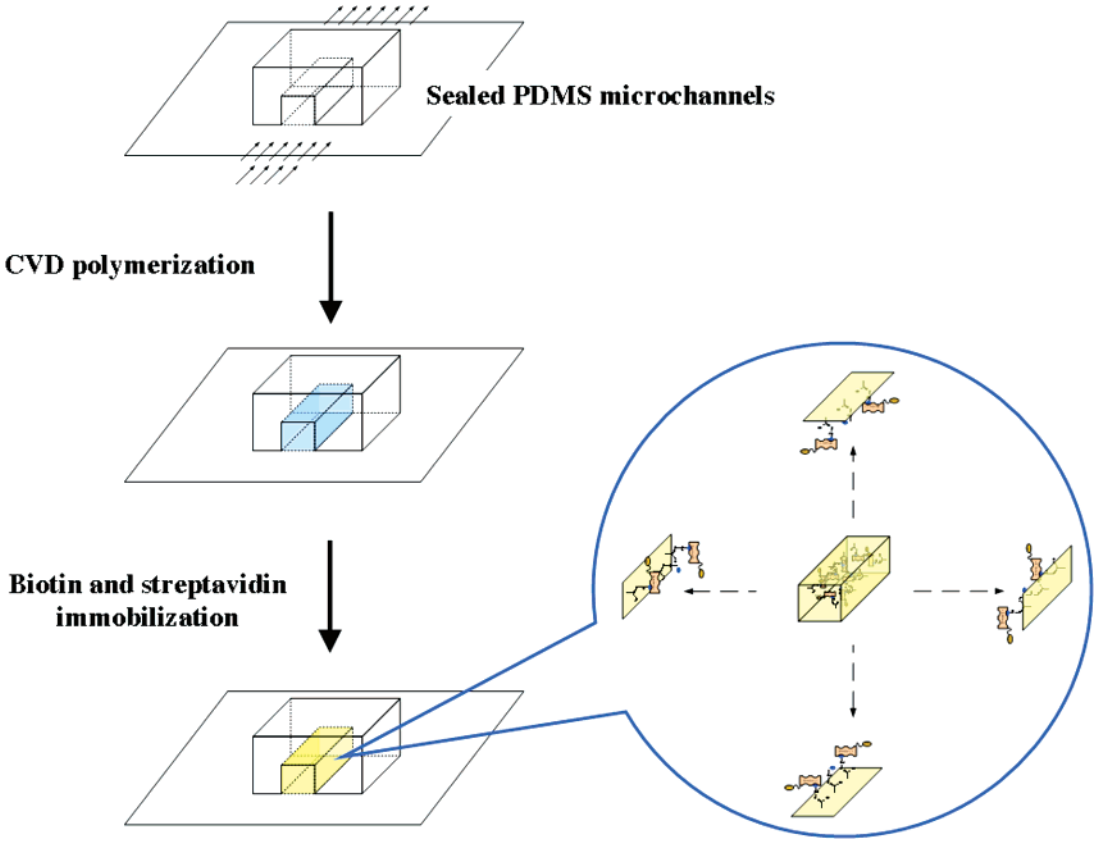

polymerization of monomers other than [2.2]paracyclophanes has been used to coated PDMS microchannels,[38] the herein described deposition of poly(*p*-xylylenes) presents a promising alternative due to the unusually low sticking coefficients encountered during CVD polymerization promoting homogeneous deposition in confined geometries.[39−41]

Conclusions

CVD polymerization of functionalized [2.2]paracyclophanes establishes a simple, but general, protocol for preparation of ultrathin polymer coatings (smaller than 100 nm). The resulting reactive coatings provide a designable interface useful for a wide range of surface modifications: active ester groups allow for immobilization of proteins; amino or carboxylic acid groups may control surface charges and electro-osmotic flows; and alkyl groups may provide hydrophobic interfaces for electrochromatographic applications.

In this study, we have used a combination of surface-analytical methods including optical and fluorescence microscopy, imaging elipsometry, atomic force microscopy, and imaging XPS to unambiguously establish the applicability of CVD coatings to the coating of confined microgeometries. Based on this study, we suggest that (1) CVD polymerization can be applied to microdevices with aspect ratios as high as 37 and results in homogeneous polymer films, which can be made of either reactive or nonreactive coatings; (2) a decrease of film thicknesses occurs toward the center of the microchannels suggesting the existence of an upper limit in the aspect ratio of the microdevices that can be coated; (3) polymer deposition is applicable to both straight and curved microchannels; (4) reactive coatings deposited within confined microgeometries provide functional groups that can sustain chemical conversion yielding homogeneous deposition of biomolecules. The fact that we have—for the first time—confirmed the deposition of reactive CVD coatings within confined microgeometries bridges a critical technological gap toward surface-modified microfluidic and nanofluidic devices with use for biosensor and "BioMEMS" applications, bioseparation, the design of high-throughput screening platforms, or the development of novel tissue constructs for regenerative medicine applications.

Acknowledgment. J.L. gratefully acknowledges support from the NSF in form of a CAREER Grant (DMR-0449462) and funding from the NSF under the MRI program (DMR-0420785). We thank Professor Larson, University of Michigan, for use of the fluorescence microscope.

Supporting Information Available: Experimental details and supporting data. This material is available free of charge via the Internet at http://pubs.acs.org.

JA057082H

(38) Gu, H.; Xu, C.; Weng, L.-T.; Xu, B. *J. Am. Chem. Soc.* **2003**, *125*, 9256−9257.
(39) Grysenko, K. P.; Tolstopyatov, E. M. *Surf. Coat. Technol.* **2004**, *180*−*181*, 450−453.
(40) Tolstopyatov, E. M. *J. Phys. D: Appl. Phys.* **2002**, *35*, 1516−1525.
(41) Tolstopyatov, E. M.; Yang, S. H.; Kim, M. C. *J. Phys. D: Appl. Phys.* **2002**, *35*, 2723−2730.